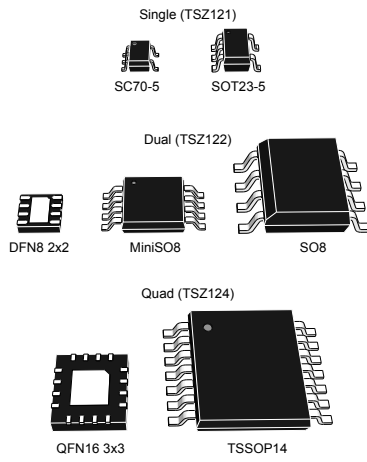


Very high accuracy (5 μ V) zero drift micropower 5 V operational amplifiers



Features

- Very high accuracy and stability: offset voltage 5 μ V max at 25 °C, 8 μ V over full temperature range (-40 °C to 125 °C)
- Rail-to-rail input and output
- Low supply voltage: 1.8 - 5.5 V
- Low power consumption: 40 μ A max. at 5 V
- Gain bandwidth product: 400 kHz
- High tolerance to ESD: 4 kV HBM
- Extended temperature range: -40 to 125 °C
- Micro-packages: SC70-5, DFN8 2x2, and QFN16 3x3

Applications

- Battery-powered applications
- Portable devices
- Signal conditioning
- Medical instrumentation

Description

The TSZ12x series of high precision operational amplifiers offer very low input offset voltages with virtually zero drift.

TSZ121 is the single version, TSZ122 the dual version, and TSZ124 the quad version, with pinouts compatible with industry standards.

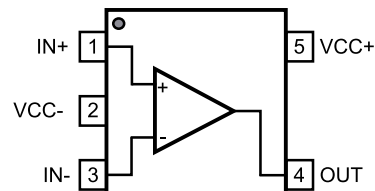
The TSZ12x series offers rail-to-rail input and output, excellent speed/power consumption ratio, and 400 kHz gain bandwidth product, while consuming less than 40 μ A at 5 V. The devices also feature an ultra-low input bias current.

These features make the TSZ12x family ideal for sensor interfaces, battery-powered applications and portable applications.

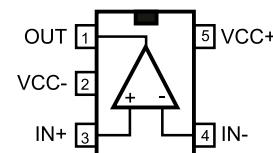
| Maturity status link | |
|-----------------------------------------------------|--------------------------------------|
| TSZ121 | |
| TSZ122 | |
| TSZ124 | |
| Related products | |
| TSV711 | Continuous-time precision amplifiers |
| TSV731 | |
| TSZ181 | Zero drift 3 MHz amplifiers |
| TSZ182 | |
| Benefits | |
| Higher accuracy without calibration | |
| Accuracy virtually unaffected by temperature change | |

1 Package pin connections

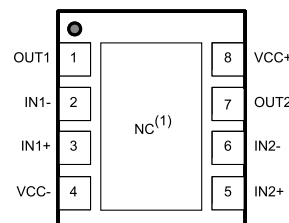
Figure 1. Pin connections for each package (top view)



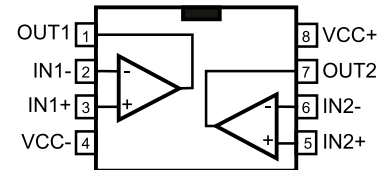
SC70-5



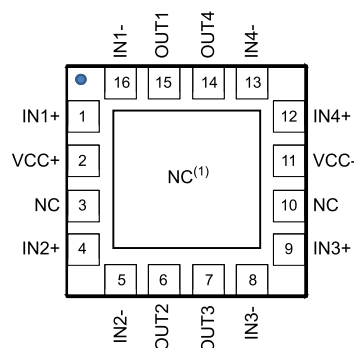
SOT23-5



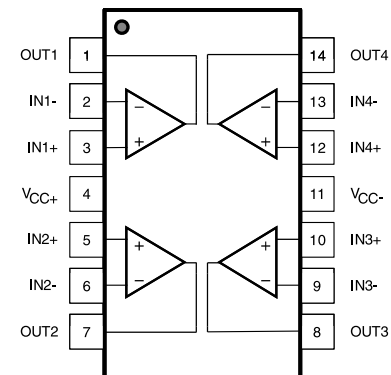
DFN8 2x2



MiniSO8 and SO8



QFN16 3x3



TSSOP14

1. The exposed pads of the DFN8 2x2 and the QFN16 3x3 can be connected to VCC- or left floating.

2

Absolute maximum ratings and operating conditions

Table 1. Absolute maximum ratings (AMR)

| Symbol | Parameter | Value | Unit |
|------------|-----------------------------------------------------------|-------------------------------------------|--------------------|
| V_{CC} | Supply voltage ⁽¹⁾ | 6 | V |
| V_{id} | Differential input voltage ⁽²⁾ | $\pm V_{CC}$ | |
| V_{in} | Input voltage ⁽³⁾ | $(V_{CC-}) - 0.2$ to $(V_{CC+}) + 0.2$ | |
| I_{in} | Input current ⁽⁴⁾ | 10 | mA |
| T_{stg} | Storage temperature | -65 to 150 | $^{\circ}\text{C}$ |
| T_j | Maximum junction temperature | 150 | |
| R_{thja} | Thermal resistance junction to ambient ^{(5) (6)} | SC70-5 | 205 |
| | | SOT23-5 | 250 |
| | | DFN8 2x2 | 57 |
| | | MiniSO8 | 190 |
| | | SO8 | 125 |
| | | QFN16 3x3 | 39 |
| | | TSSOP14 | 100 |
| ESD | HBM: human body model ⁽⁷⁾ | 4 | kV |
| | MM: machine model ⁽⁸⁾ | 300 | V |
| | CDM: charged device model ⁽⁹⁾ | 1.5 | kV |
| | Latch-up immunity | 200 | mA |

1. All voltage values, except the differential voltage are with respect to the network ground terminal.
2. The differential voltage is the non-inverting input terminal with respect to the inverting input terminal.
3. $V_{CC} - V_{in}$ must not exceed 6 V, V_{in} must not exceed 6 V
4. Input current must be limited by a resistor in series with the inputs.
5. R_{th} are typical values.
6. Short-circuits can cause excessive heating and destructive dissipation.
7. Human body model: 100 pF discharged through a 1.5 k Ω resistor between two pins of the device, done for all couples of pin combinations with other pins floating.
8. Machine model: a 200 pF cap is charged to the specified voltage, then discharged directly between two pins of the device with no external series resistor (internal resistor < 5 Ω), done for all couples of pin combinations with other pins floating.
9. Charged device model: all pins plus package are charged together to the specified voltage and then discharged directly to ground.

Table 2. Operating conditions

| Symbol | Parameter | Value | Unit |
|------------|--------------------------------------|----------------------------------------|--------------------|
| V_{CC} | Supply voltage | 1.8 to 5.5 | V |
| V_{icm} | Common mode input voltage range | $(V_{CC-}) - 0.1$ to $(V_{CC+}) + 0.1$ | |
| T_{oper} | Operating free air temperature range | -40 to 125 | $^{\circ}\text{C}$ |

3 Electrical characteristics

Table 3. Electrical characteristics at $V_{CC+} = 1.8$ V with $V_{CC-} = 0$ V, $V_{icm} = V_{CC}/2$, $T = 25^\circ C$, and $R_L = 10$ k Ω connected to $V_{CC}/2$ (unless otherwise specified)

| Symbol | Parameter | Conditions | Min. | Typ. | Max. | Unit |
|--------------------------|-------------------------------------------------------------------------------------------------------------------------------------------------|---------------------------------------------------------------------|------|------|--------------------|----------------|
| DC performance | | | | | | |
| V_{io} | Input offset voltage | $T = 25^\circ C$ | | 1 | 5 | μV |
| | | $-40^\circ C < T < 125^\circ C$ | | | 8 | |
| $\Delta V_{io}/\Delta T$ | Input offset voltage drift ⁽¹⁾ | $-40^\circ C < T < 125^\circ C$ | | 10 | 30 | nV/ $^\circ C$ |
| I_{ib} | Input bias current ($V_{out} = V_{CC}/2$) | $T = 25^\circ C$ | | 50 | 200 ⁽²⁾ | pA |
| | | $-40^\circ C < T < 125^\circ C$ | | | 300 ⁽²⁾ | |
| I_{io} | Input offset current ($V_{out} = V_{CC}/2$) | $T = 25^\circ C$ | | 100 | 400 ⁽²⁾ | |
| | | $-40^\circ C < T < 125^\circ C$ | | | 600 ⁽²⁾ | |
| CMR | Common mode rejection ratio, 20 log $(\Delta V_{icm}/\Delta V_{io})$, $V_{ic} = 0$ V to V_{CC} , $V_{out} = V_{CC}/2$, $R_L > 1$ M Ω | $T = 25^\circ C$ | 110 | 122 | | dB |
| | | $-40^\circ C < T < 125^\circ C$ | 110 | | | |
| A_{vd} | Large signal voltage gain, $V_{out} = 0.5$ V to $(V_{CC} - 0.5)$ V | $T = 25^\circ C$ | 118 | 135 | | |
| | | $-40^\circ C < T < 125^\circ C$ | 110 | | | |
| V_{OH} | High-level output voltage | $T = 25^\circ C$ | | | 30 | mV |
| | | $-40^\circ C < T < 125^\circ C$ | | | 70 | |
| V_{OL} | Low-level output voltage | $T = 25^\circ C$ | | | 30 | |
| | | $-40^\circ C < T < 125^\circ C$ | | | 70 | |
| I_{out} | I_{sink} ($V_{out} = V_{CC}$) | $T = 25^\circ C$ | 7 | 8 | | mA |
| | | $-40^\circ C < T < 125^\circ C$ | 6 | | | |
| | I_{source} ($V_{out} = 0$ V) | $T = 25^\circ C$ | 5 | 7 | | |
| | | $-40^\circ C < T < 125^\circ C$ | 4 | | | |
| I_{CC} | Supply current (per amplifier, $V_{out} = V_{CC}/2$, $R_L > 1$ M Ω) | $T = 25^\circ C$ | | 28 | 40 | μA |
| | | $-40^\circ C < T < 125^\circ C$ | | | 40 | |
| AC performance | | | | | | |
| GBP | Gain bandwidth product | $R_L = 10$ k Ω , $C_L = 100$ pF | | 400 | | kHz |
| F_u | Unity gain frequency | | | 300 | | |
| ϕ_m | Phase margin | | | 55 | | |
| G_m | Gain margin | | | 17 | | |
| SR | Slew rate ⁽³⁾ | | | 0.17 | | |
| t_s | Setting time | To 0.1 %, $V_{in} = 1$ Vp-p, $R_L = 10$ k Ω , $C_L = 100$ pF | | 50 | | μs |
| e_n | Equivalent input noise voltage | $f = 1$ kHz | | 60 | | nV/\sqrt{Hz} |
| | | $f = 10$ kHz | | 60 | | |
| $\int e_n$ | Low-frequency peak-to-peak input noise | Bandwidth, $f = 0.1$ to 10 Hz | | 1.1 | | μVpp |
| C_s | Channel separation | $f = 100$ Hz | | 120 | | dB |

| Symbol | Parameter | Conditions | Min. | Typ. | Max. | Unit |
|------------|---------------------|---------------------|------|------|------|------|
| t_{init} | Initialization time | T = 25 °C | 50 | | | μs |
| | | -40 °C < T < 125 °C | 100 | | | |

1. See [Section 5.5 Input offset voltage drift over temperature](#). Input offset measurements are performed on x100 gain configuration. The amplifiers and the gain setting resistors are at the same temperature.
2. Guaranteed by design
3. Slew rate value is calculated as the average between positive and negative slew rates.

Table 4. Electrical characteristics at $V_{CC+} = 3.3$ V with $V_{CC-} = 0$ V, $V_{icm} = V_{CC}/2$, $T = 25$ °C, and $R_L = 10$ kΩ connected to $V_{CC}/2$ (unless otherwise specified)

| Symbol | Parameter | Conditions | Min. | Typ. | Max. | Unit |
|--------------------------|-----------------------------------------------------------------------------------------------------------------------------------------|------------------------------------------------------------|------|--------------------|------|---------|
| DC performance | | | | | | |
| V_{io} | Input offset voltage | T = 25 °C | | 1 | 5 | μV |
| | | -40 °C < T < 125 °C | | 8 | | |
| $\Delta V_{io}/\Delta T$ | Input offset voltage drift ⁽¹⁾ | -40 °C < T < 125 °C | 10 | 30 | | nV/°C |
| I_{ib} | Input bias current ($V_{out} = V_{CC}/2$) | T = 25 °C | 60 | 200 ⁽²⁾ | | pA |
| | | -40 °C < T < 125 °C | | 300 ⁽²⁾ | | |
| I_{io} | Input offset current ($V_{out} = V_{CC}/2$) | T = 25 °C | 120 | 400 ⁽²⁾ | | |
| | | -40 °C < T < 125 °C | | 600 ⁽²⁾ | | |
| CMR | Common mode rejection ratio, 20 log $(\Delta V_{icm}/\Delta V_{io})$, $V_{ic} = 0$ V to V_{CC} , $V_{out} = V_{CC}/2$, $R_L > 1$ MΩ | T = 25 °C | 115 | 128 | | dB |
| | | -40 °C < T < 125 °C | 115 | | | |
| A_{vd} | Large signal voltage gain, $V_{out} = 0.5$ V to $(V_{CC} - 0.5)$ V | T = 25 °C | 118 | 135 | | |
| | | -40 °C < T < 125 °C | 110 | | | |
| V_{OH} | High-level output voltage | T = 25 °C | | | 30 | mV |
| | | -40 °C < T < 125 °C | | | 70 | |
| V_{OL} | Low-level output voltage | T = 25 °C | | | 30 | |
| | | -40 °C < T < 125 °C | | | 70 | |
| I_{out} | I_{sink} ($V_{out} = V_{CC}$) | T = 25 °C | 15 | 18 | | mA |
| | | -40 °C < T < 125 °C | 12 | | | |
| | I_{source} ($V_{out} = 0$ V) | T = 25 °C | 14 | 16 | | |
| | | -40 °C < T < 125 °C | 10 | | | |
| I_{cc} | Supply current (per amplifier, $V_{out} = V_{CC}/2$, $R_L > 1$ MΩ) | T = 25 °C | | 29 | 40 | μA |
| | | -40 °C < T < 125 °C | | | 40 | |
| AC performance | | | | | | |
| GBP | Gain bandwidth product | $R_L = 10$ kΩ, $C_L = 100$ pF | | 400 | | kHz |
| F_u | Unity gain frequency | | | 300 | | |
| ϕ_m | Phase margin | | | 56 | | Degrees |
| G_m | Gain margin | | | 19 | | dB |
| SR | Slew rate ⁽³⁾ | | | 0.19 | | V/μs |
| t_s | Setting time | To 0.1 %, $V_{in} = 1$ Vp-p, $R_L = 10$ kΩ, $C_L = 100$ pF | | 50 | | μs |

| Symbol | Parameter | Conditions | Min. | Typ. | Max. | Unit |
|------------|----------------------------------------|------------------------------------------------|------|------|------|------------------------------|
| e_n | Equivalent input noise voltage | $f = 1 \text{ kHz}$ | 40 | | | $\text{nV}/\sqrt{\text{Hz}}$ |
| | | $f = 10 \text{ kHz}$ | 40 | | | |
| $\int e_n$ | Low-frequency peak-to-peak input noise | Bandwidth, $f = 0.1 \text{ to } 10 \text{ Hz}$ | 0.8 | | | μVpp |
| C_s | Channel separation | $f = 100 \text{ Hz}$ | 120 | | | dB |
| t_{init} | Initialization time | $T = 25^\circ\text{C}$ | 50 | | | μs |
| | | $-40^\circ\text{C} < T < 125^\circ\text{C}$ | 100 | | | |

1. See [Section 5.5 Input offset voltage drift over temperature](#). Input offset measurements are performed on $\times 100$ gain configuration. The amplifiers and the gain setting resistors are at the same temperature.
2. Guaranteed by design
3. Slew rate value is calculated as the average between positive and negative slew rates.

Table 5. Electrical characteristics at $V_{CC+} = 5 \text{ V}$ with $V_{CC-} = 0 \text{ V}$, $V_{icm} = V_{CC}/2$, $T = 25^\circ\text{C}$, and $R_L = 10 \text{ k}\Omega$ connected to $V_{CC}/2$ (unless otherwise specified)

| Symbol | Parameter | Conditions | Min. | Typ. | Max. | Unit |
|--------------------------|-------------------------------------------------------------------------------------------------------------------------------------------------------------------------|------------------------------------------------------|------|------|--------------------|----------------------------|
| DC performance | | | | | | |
| V_{io} | Input offset voltage | $T = 25^\circ\text{C}$ | | 1 | 5 | μV |
| | | $-40^\circ\text{C} < T < 125^\circ\text{C}$ | | 8 | | |
| $\Delta V_{io}/\Delta T$ | Input offset voltage drift ⁽¹⁾ | $-40^\circ\text{C} < T < 125^\circ\text{C}$ | | 10 | 30 | $\text{nV}/^\circ\text{C}$ |
| I_{ib} | Input bias current ($V_{out} = V_{CC}/2$) | $T = 25^\circ\text{C}$ | | 70 | 200 ⁽²⁾ | pA |
| | | $-40^\circ\text{C} < T < 125^\circ\text{C}$ | | | 300 ⁽²⁾ | |
| I_{io} | Input offset current ($V_{out} = V_{CC}/2$) | $T = 25^\circ\text{C}$ | | 140 | 400 ⁽²⁾ | pA |
| | | $-40^\circ\text{C} < T < 125^\circ\text{C}$ | | | 600 ⁽²⁾ | |
| CMR | Common mode rejection ratio, 20 log $(\Delta V_{icm}/\Delta V_{io})$, $V_{ic} = 0 \text{ V}$ to V_{CC} , $V_{out} = V_{CC}/2$, $R_L > 1 \text{ M}\Omega$ | $T = 25^\circ\text{C}$ | 115 | 136 | | |
| | | $-40^\circ\text{C} < T < 125^\circ\text{C}$ | 115 | | | |
| SVR | Supply voltage rejection ratio, 20 log $(\Delta V_{CC}/\Delta V_{io})$, $V_{CC} = 1.8 \text{ V}$ to 5.5 V , $V_{out} = V_{CC}/2$, $R_L > 1 \text{ M}\Omega$ | $T = 25^\circ\text{C}$ | 120 | 140 | | dB |
| | | $-40^\circ\text{C} < T < 125^\circ\text{C}$ | 120 | | | |
| A_{vd} | Large signal voltage gain, $V_{out} = 0.5 \text{ V}$ to $(V_{CC} - 0.5 \text{ V})$ | $T = 25^\circ\text{C}$ | 120 | 135 | | dB |
| | | $-40^\circ\text{C} < T < 125^\circ\text{C}$ | 110 | | | |
| $EMIRR$ ⁽³⁾ | EMI rejection rate = $-20 \log (V_{RFpeak}/\Delta V_{io})$ | $V_{RF} = 100 \text{ mV}_p$, $f = 400 \text{ MHz}$ | | 84 | | |
| | | $V_{RF} = 100 \text{ mV}_p$, $f = 900 \text{ MHz}$ | | 87 | | |
| | | $V_{RF} = 100 \text{ mV}_p$, $f = 1800 \text{ MHz}$ | | 90 | | |
| | | $V_{RF} = 100 \text{ mV}_p$, $f = 2400 \text{ MHz}$ | | 91 | | |
| V_{OH} | High-level output voltage | $T = 25^\circ\text{C}$ | | | 30 | mV |
| | | $-40^\circ\text{C} < T < 125^\circ\text{C}$ | | | 70 | |
| V_{OL} | Low-level output voltage | $T = 25^\circ\text{C}$ | | | 30 | mV |
| | | $-40^\circ\text{C} < T < 125^\circ\text{C}$ | | | 70 | |

| Symbol | Parameter | Conditions | Min. | Typ. | Max. | Unit |
|-----------------------|-----------------------------------------------------------------------------------|----------------------------------------------------------------------------------------------|------|------|------|---------|
| I _{out} | I _{sink} ($V_{out} = V_{CC}$) | T = 25 °C | 15 | 18 | | mA |
| | | -40 °C < T < 125 °C | 14 | | | |
| | I _{source} ($V_{out} = 0$ V) | T = 25 °C | 14 | 17 | | |
| | | -40 °C < T < 125 °C | 12 | | | |
| I _{CC} | Supply current (per amplifier, $V_{out} = V_{CC}/2$, $R_L > 1 \text{ M}\Omega$) | T = 25 °C | | 31 | 40 | μA |
| | | -40 °C < T < 125 °C | | | 40 | |
| AC performance | | | | | | |
| GBP | Gain bandwidth product | $R_L = 10 \text{ k}\Omega$, $C_L = 100 \text{ pF}$ | | 400 | | kHz |
| F _u | Unity gain frequency | | | 300 | | |
| φm | Phase margin | | | 53 | | Degrees |
| G _m | Gain margin | | | 19 | | dB |
| SR | Slew rate ⁽⁴⁾ | | | 0.19 | | V/μs |
| t _s | Setting time | To 0.1 %, $V_{in} = 100 \text{ mVp-p}$, $R_L = 10 \text{ k}\Omega$, $C_L = 100 \text{ pF}$ | | 10 | | μs |
| e _n | Equivalent input noise voltage | f = 1 kHz | | 37 | | nV/√Hz |
| | | f = 10 kHz | | 37 | | |
| ∫e _n | Low-frequency peak-to-peak input noise | Bandwidth, f = 0.1 to 10 Hz | | 0.75 | | μVpp |
| C _s | Channel separation | f = 100 Hz | | 120 | | dB |
| t _{init} | Initialization time | T = 25 °C | | 50 | | μs |
| | | -40 °C < T < 125 °C | | 100 | | |

1. See [Section 5.5 Input offset voltage drift over temperature](#). Input offset measurements are performed on x100 gain configuration. The amplifiers and the gain setting resistors are at the same temperature.

2. Guaranteed by design

3. Tested on SC70-5 package

4. Slew rate value is calculated as the average between positive and negative slew rates.

4 Electrical characteristic curves

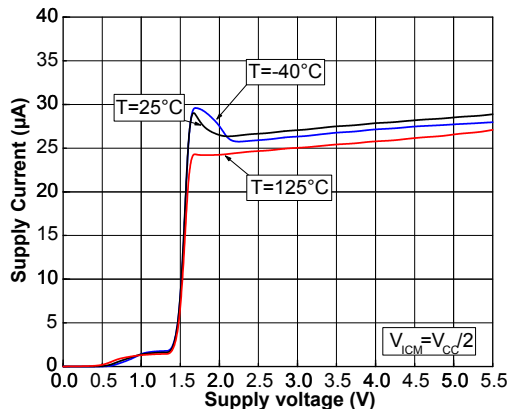
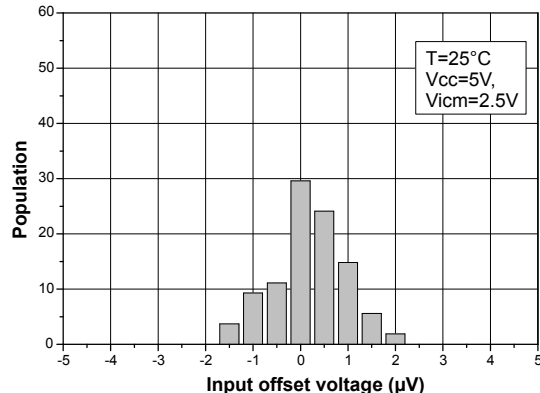
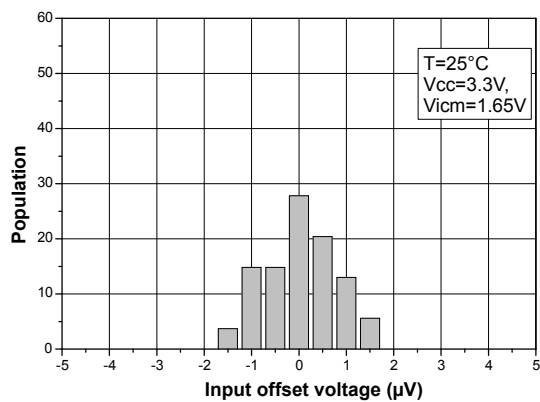
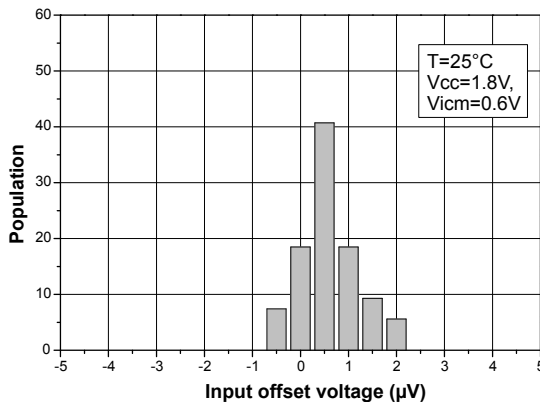
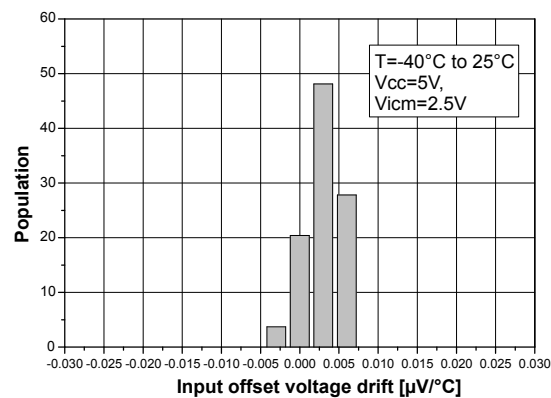
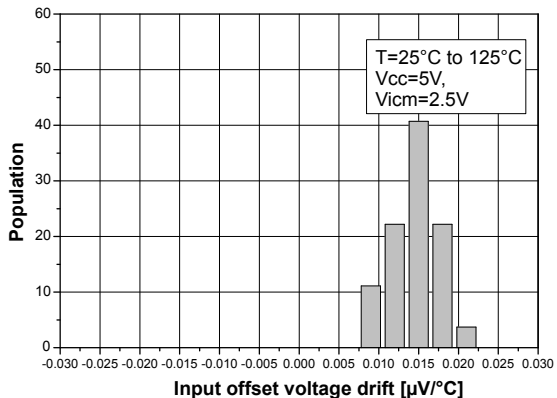
Figure 2. Supply current vs. supply voltage**Figure 3.** Input offset voltage distribution at $V_{\text{CC}} = 5\text{ V}$ **Figure 4.** Input offset voltage distribution at $V_{\text{CC}} = 3.3\text{ V}$ **Figure 5.** Input offset voltage distribution at $V_{\text{CC}} = 1.8\text{ V}$ **Figure 6.** V_{IO} temperature co-efficient distribution (-40° C to 25° C)**Figure 7.** V_{IO} temperature co-efficient distribution (25° C to 125° C)

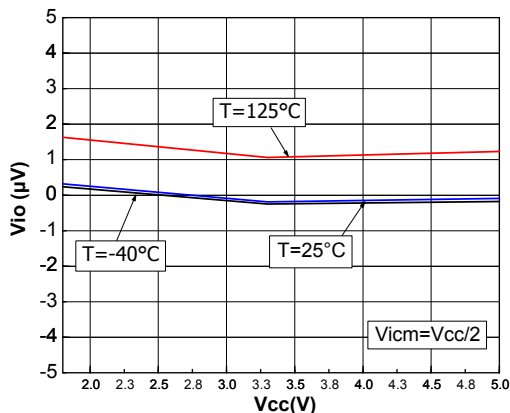
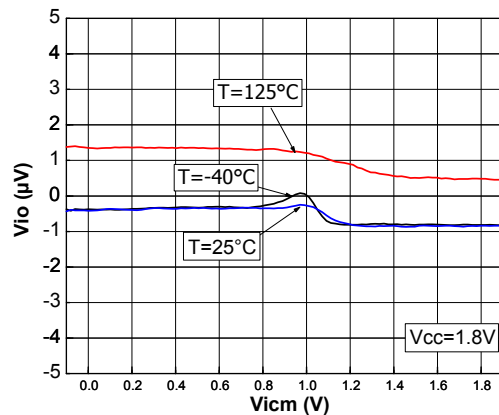
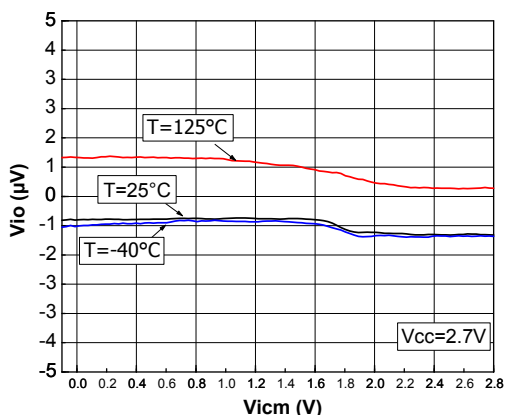
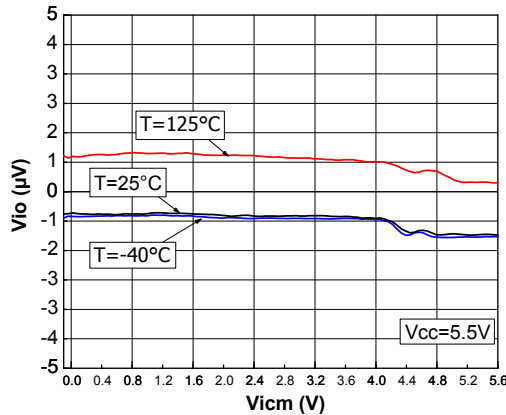
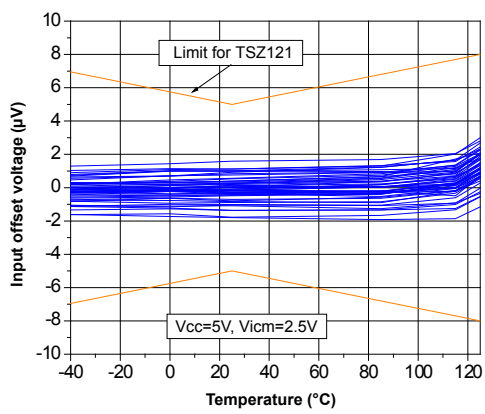
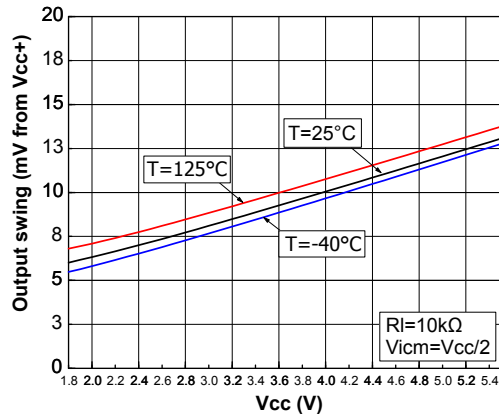
Figure 8. Input offset voltage vs. supply voltage

Figure 9. Input offset voltage vs. input common-mode at $V_{CC} = 1.8 \text{ V}$

Figure 10. Input offset voltage vs. input common-mode at $V_{CC} = 2.7 \text{ V}$

Figure 11. Input offset voltage vs. input common-mode at $V_{CC} = 5.5 \text{ V}$

Figure 12. Input offset voltage vs. temperature

Figure 13. V_{OH} vs. supply voltage


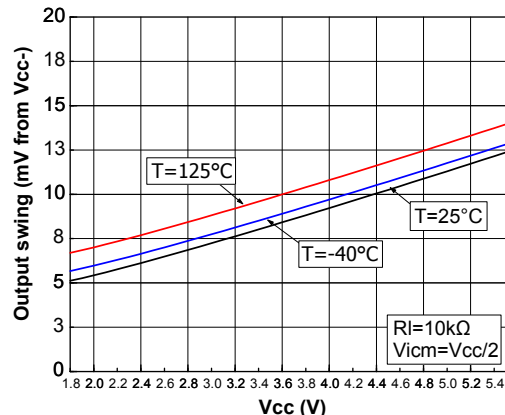
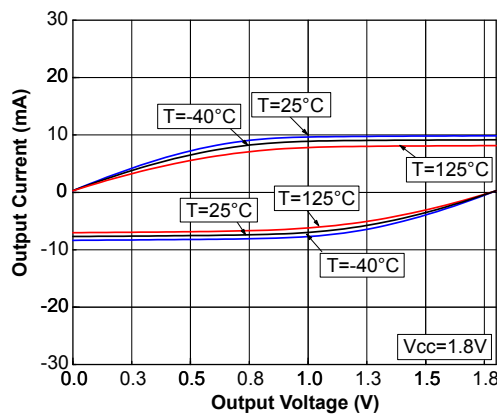
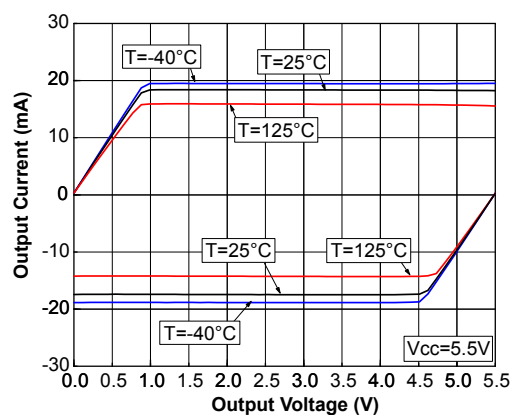
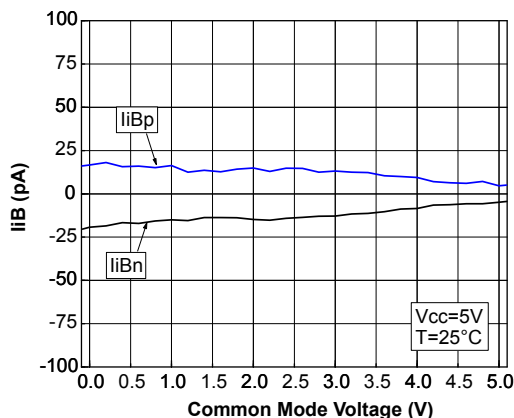
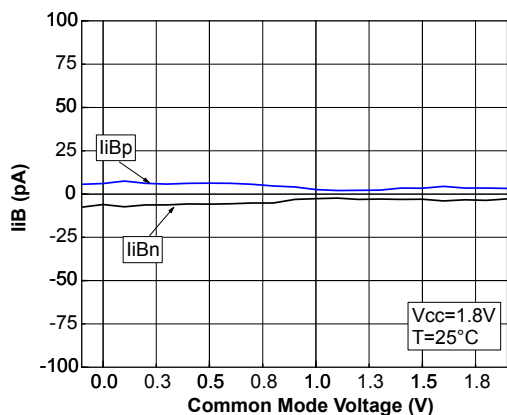
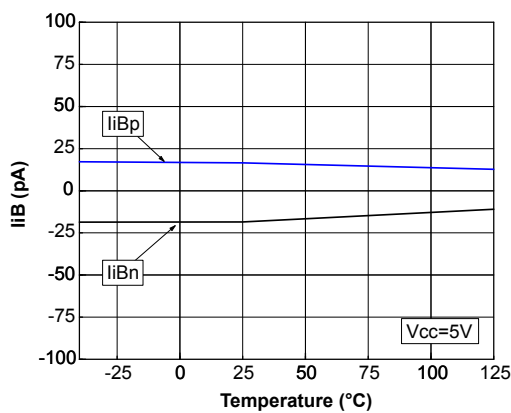
Figure 14. V_{OL} vs. supply voltage

Figure 15. Output current vs. output voltage at $V_{CC} = 1.8$ V

Figure 16. Output current vs. output voltage at $V_{CC} = 5.5$ V

Figure 17. Input bias current vs. common mode at $V_{CC} = 5$ V

Figure 18. Input bias current vs. common mode at $V_{CC} = 1.8$ V

Figure 19. Input bias current vs. temperature at $V_{CC} = 5$ V


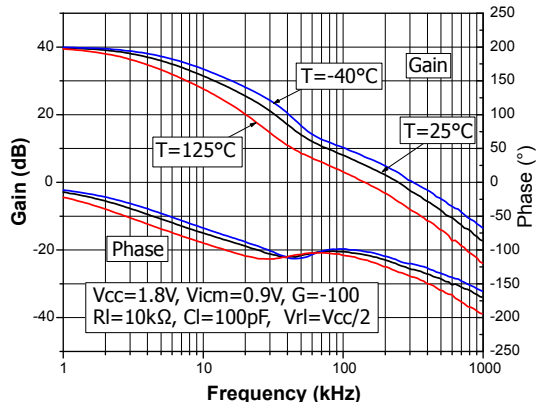
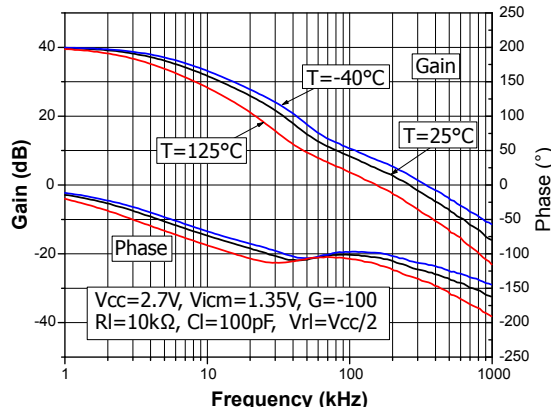
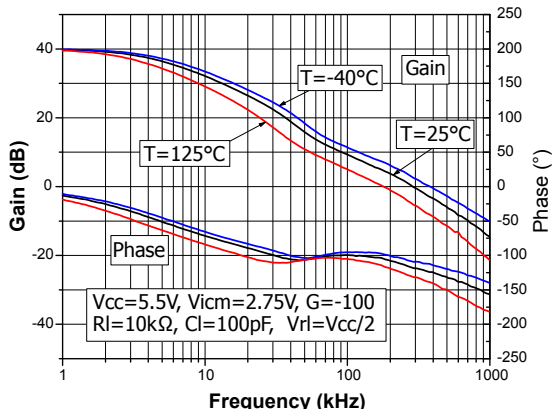
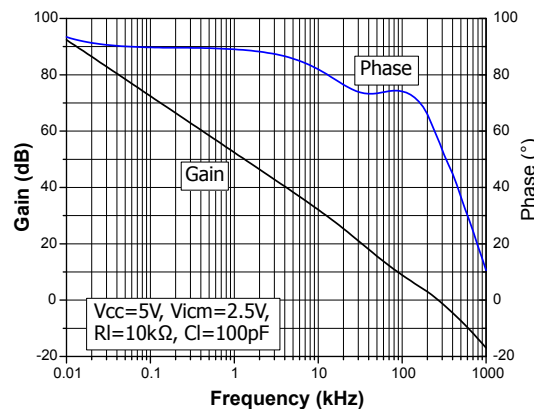
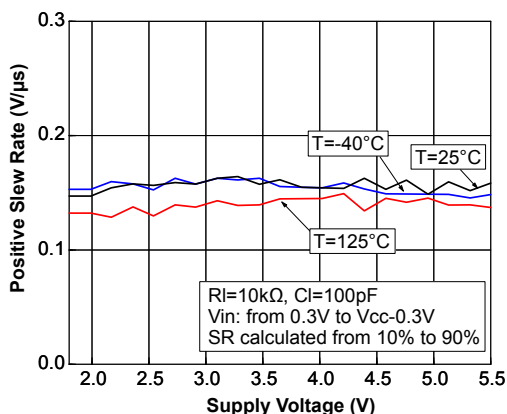
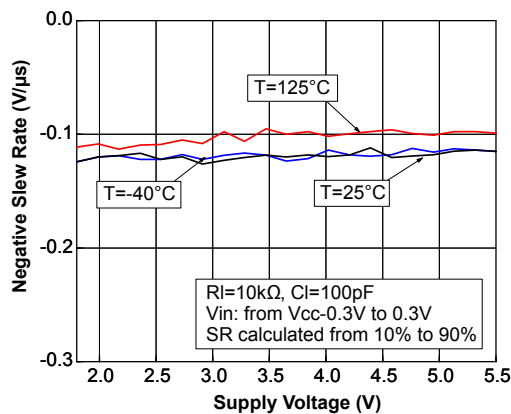
Figure 20. Bode diagram at $V_{CC} = 1.8 \text{ V}$

Figure 21. Bode diagram at $V_{CC} = 2.7 \text{ V}$

Figure 22. Bode diagram at $V_{CC} = 5.5 \text{ V}$

Figure 23. Open loop gain vs. frequency

Figure 24. Positive slew rate vs. supply voltage

Figure 25. Negative slew rate vs. supply voltage


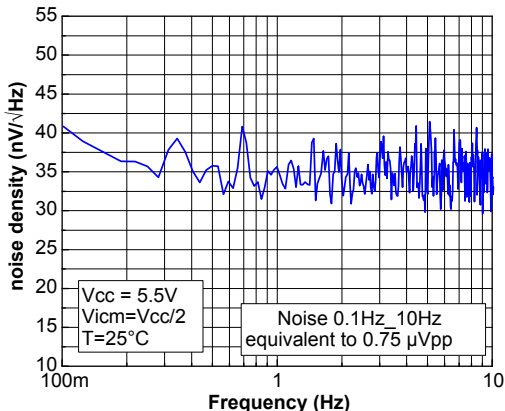
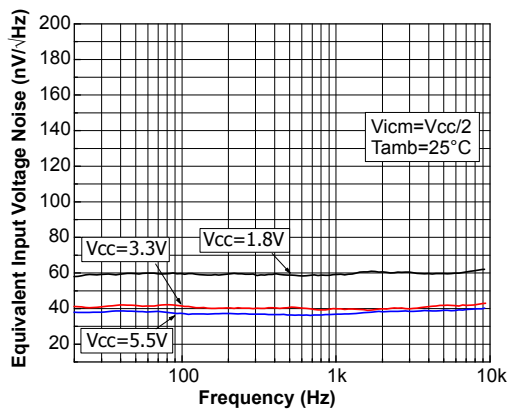
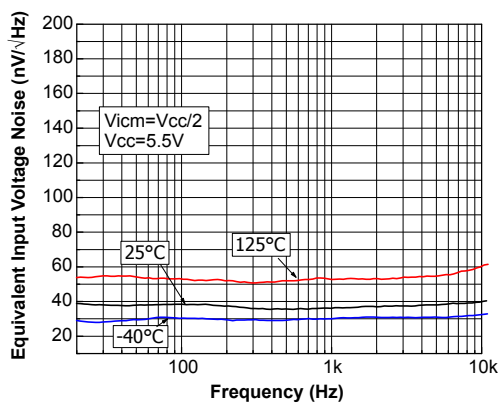
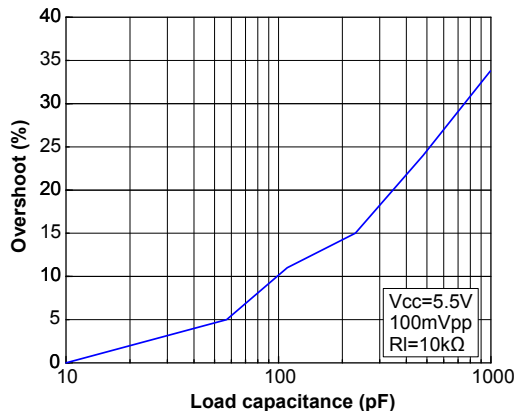
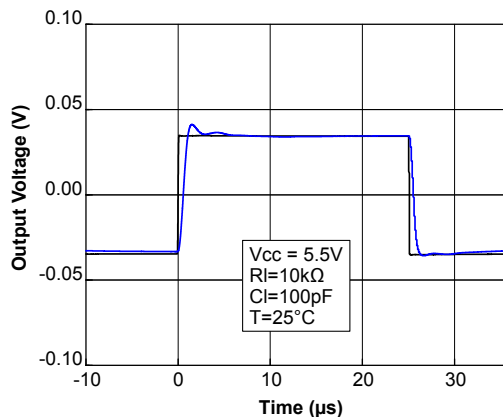
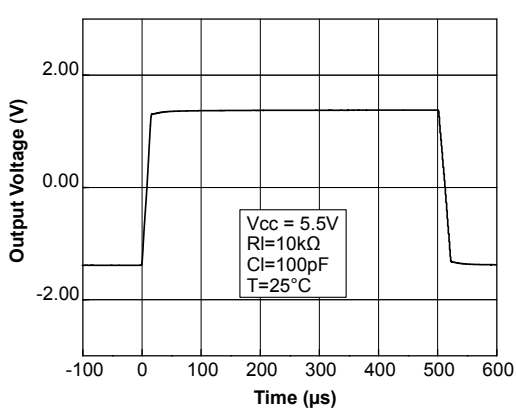
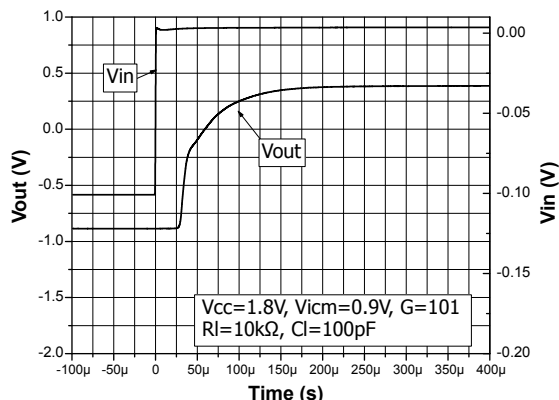
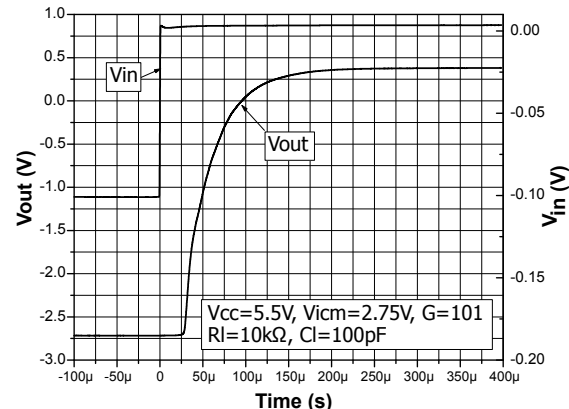
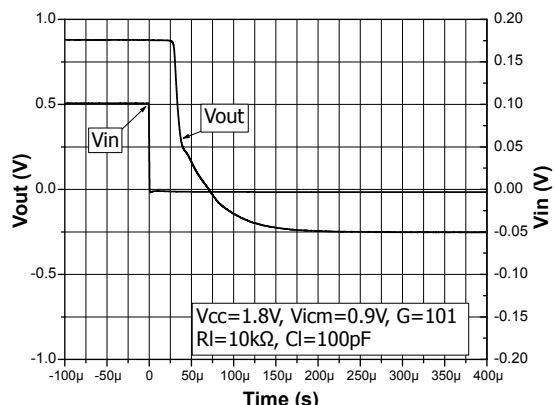
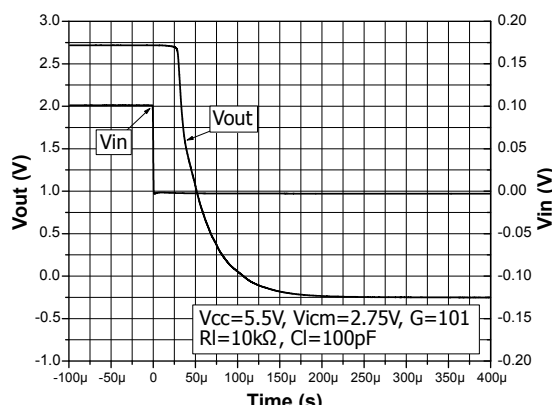
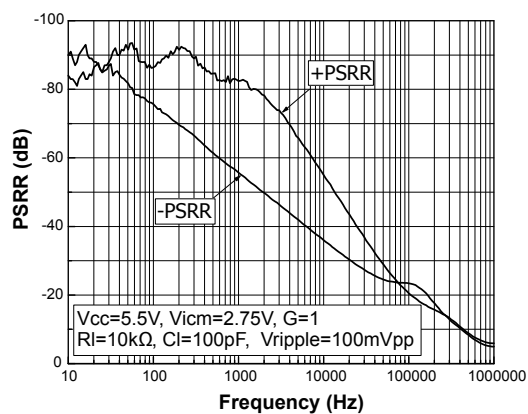
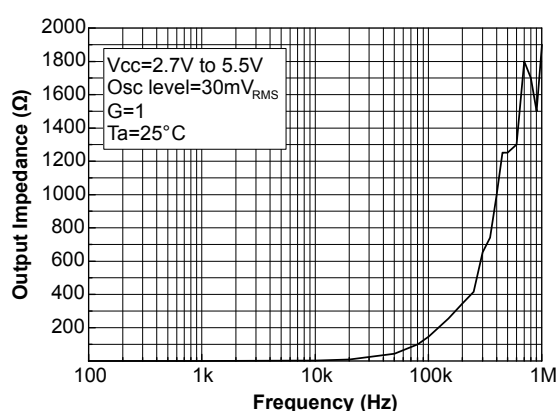
Figure 26. 0.1 Hz to 10 Hz noise

Figure 27. Noise vs. frequency

Figure 28. Noise vs. frequency and temperature

Figure 29. Output overshoot vs. load capacitance

Figure 30. Small signal

Figure 31. Large signal


Figure 32. Positive overvoltage recovery at $V_{CC} = 1.8 \text{ V}$

Figure 33. Positive overvoltage recovery at $V_{CC} = 5 \text{ V}$

Figure 34. Negative overvoltage recovery at $V_{CC} = 1.8 \text{ V}$

Figure 35. Negative overvoltage recovery at $V_{CC} = 5 \text{ V}$

Figure 36. PSRR vs. frequency

Figure 37. Output impedance vs. frequency


5 Application information

5.1 Operation theory

The TSZ121, TSZ122, and TSZ124 are high precision CMOS devices. They achieve a low offset drift and no 1/f noise thanks to their chopper architecture. Chopper-stabilized amps constantly correct low-frequency errors across the inputs of the amplifier.

Chopper-stabilized amplifiers can be explained with respect to:

- Time domain
- Frequency domain

5.1.1 Time domain

The basis of the chopper amplifier is realized in two steps. These steps are synchronized thanks to a clock running at 400 kHz.

Figure 38. Block diagram in the time domain (step 1)

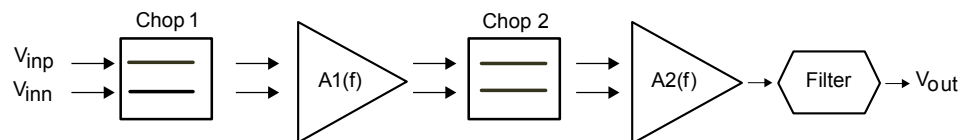


Figure 39. Block diagram in the time domain (step 2)

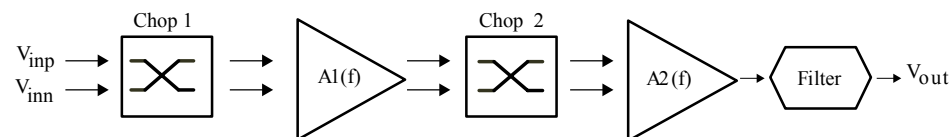


Figure 38. Block diagram in the time domain (step 1) shows step 1, the first clock cycle, where V_{io} is amplified in the normal way.

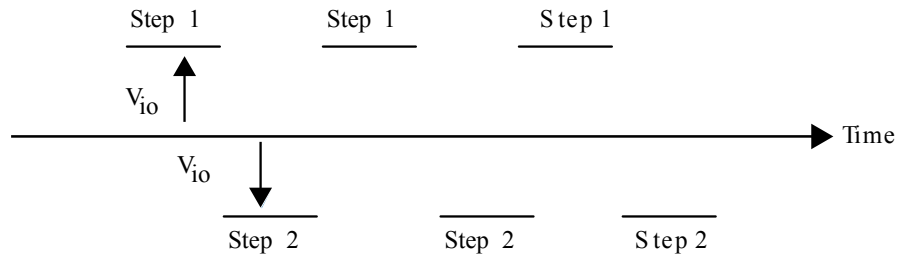
Figure 39. Block diagram in the time domain (step 2) shows step 2, the second clock cycle, where Chop1 and Chop2 swap paths. At this time, the V_{io} is amplified in a reverse way as compared to step 1.

At the end of these two steps, the average V_{io} is close to zero.

The $A2(f)$ amplifier has a small impact on the V_{io} because the V_{io} is expressed as the input offset and is consequently divided by $A1(f)$.

In the time domain, the offset part of the output signal before filtering is shown in Figure 40. V_{io} cancellation principle.

Figure 40. V_{io} cancellation principle



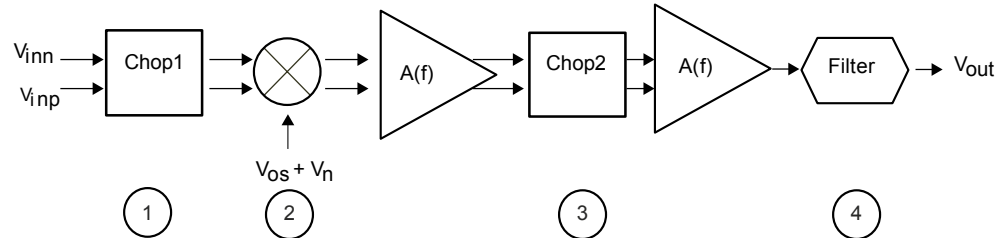
The low pass filter averages the output value resulting in the cancellation of the V_{io} offset.

The 1/f noise can be considered as an offset in low frequency and it is canceled like the V_{io} , thanks to the chopper technique.

5.1.2 Frequency domain

The frequency domain gives a more accurate vision of chopper-stabilized amplifier architecture.

Figure 41. Block diagram in the frequency domain



The modulation technique transposes the signal to a higher frequency where there is no 1/f noise, and demodulate it back after amplification.

1. According to Figure 41. Block diagram in the frequency domain, the input signal V_{in} is modulated once (Chop1) so all the input signal is transposed to the high frequency domain.
2. The amplifier adds its own error (V_{io} (output offset voltage) + the noise V_n (1/f noise)) to this modulated signal.
3. This signal is then demodulated (Chop2), but since the noise and the offset are modulated only once, they are transposed to the high frequency, leaving the output signal of the amplifier without any offset and low frequency noise. Consequently, the input signal is amplified with a very low offset and 1/f noise.
4. To get rid of the high frequency part of the output signal (which is useless) a low pass filter is implemented. To further suppress the remaining ripple down to a desired level, another low pass filter may be added externally on the output of the TSZ121, TSZ122, or TSZ124 device.

5.2 Operating voltages

TSZ121, TSZ122, and TSZ124 devices can operate from 1.8 to 5.5 V. The parameters are fully specified for 1.8 V, 3.3 V, and 5 V power supplies. However, the parameters are very stable in the full V_{CC} range and several characterization curves show the TSZ121, TSZ122, and TSZ124 device characteristics at 1.8 V and 5.5 V. Additionally, the main specifications are guaranteed in extended temperature ranges from -40 to 125 ° C.

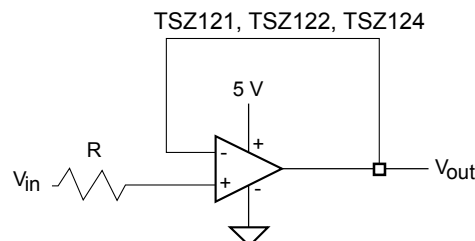
5.3 Input pin voltage ranges

TSZ121, TSZ122, and TSZ124 devices have internal ESD diode protection on the inputs. These diodes are connected between the input and each supply rail to protect the input MOSFETs from electrical discharge.

If the input pin voltage exceeds the power supply by 0.5 V, the ESD diodes become conductive and excessive current can flow through them. Without limitation this over current can damage the device.

In this case, it is important to limit the current to 10 mA, by adding resistance on the input pin, as described in [Figure 42. Input current limitation](#).

Figure 42. Input current limitation



5.4 Rail-to-rail input

TSZ121, TSZ122, and TSZ124 devices have a rail-to-rail input, and the input common mode range is extended from (V_{CC-}) - 0.1 V to (V_{CC+}) + 0.1 V.

5.5 Input offset voltage drift over temperature

The maximum input voltage drift variation over temperature is defined as the offset variation related to the offset value measured at 25 °C. The operational amplifier is one of the main circuits of the signal conditioning chain, and the amplifier input offset is a major contributor to the chain accuracy. The signal chain accuracy at 25 °C can be compensated during production at application level. The maximum input voltage drift over temperature enables the system designer to anticipate the effect of temperature variations.

The maximum input voltage drift over temperature is computed using [Equation 1](#).

Equation 1

$$\frac{\Delta V_{io}}{\Delta T} = \max \left| \frac{V_{io}(T) - V_{io}(25^\circ\text{C})}{T - 25^\circ\text{C}} \right|$$

Where T = -40 °C and 125 °C.

The TSZ121, TSZ122, and TSZ124 datasheet maximum value is guaranteed by measurements on a representative sample size ensuring a C_{pk} (process capability index) greater than 1.3.

5.6 Rail-to-rail output

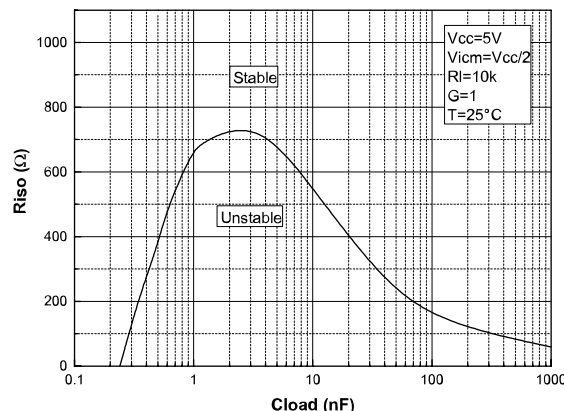
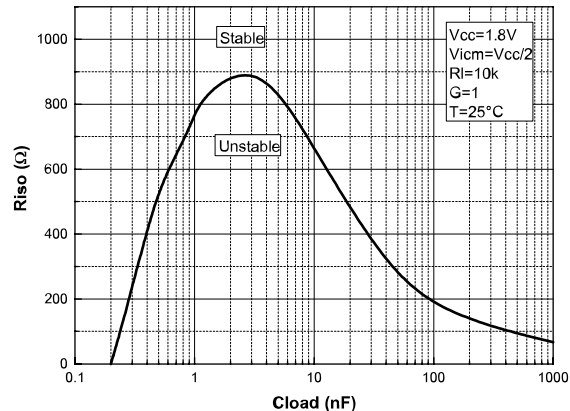
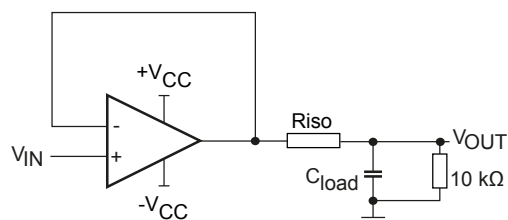
The operational amplifier output levels can go close to the rails: to a maximum of 30 mV above and below the rail when connected to a 10 kΩ resistive load to V_{CC}/2.

5.7 Capacitive load

Driving large capacitive loads can cause stability problems. Increasing the load capacitance produces gain peaking in the frequency response, with overshoot and ringing in the step response. It is usually considered that with a gain peaking higher than 2.3 dB an op amp might become unstable.

Generally, the unity gain configuration is the worst case for stability and the ability to drive large capacitive loads.

[Figure 43. Stability criteria with a serial resistor at V_{DD} = 5 V](#) and [Figure 44. Stability criteria with a serial resistor at V_{DD} = 1.8 V](#) show the serial resistor that must be added to the output, to make a system stable. [Figure 45. Test configuration for Riso](#) shows the test configuration using an isolation resistor, Riso.

Figure 43. Stability criteria with a serial resistor at $V_{DD} = 5 \text{ V}$ **Figure 44. Stability criteria with a serial resistor at $V_{DD} = 1.8 \text{ V}$** **Figure 45. Test configuration for Riso**

5.8 PCB layout recommendations

Particular attention must be paid to the layout of the PCB, tracks connected to the amplifier, load, and power supply. The power and ground traces are critical as they must provide adequate energy and grounding for all circuits. Good practice is to use short and wide PCB traces to minimize voltage drops and parasitic inductance. In addition, to minimize parasitic impedance over the entire surface, a multi-via technique that connects the bottom and top layer ground planes together in many locations is often used.

The copper traces that connect the output pins to the load and supply pins should be as wide as possible to minimize trace resistance.

5.9 Optimized application recommendation

TSZ121, TSZ122, and TSZ124 devices are based on chopper architecture. As they are switched devices, it is strongly recommended to place a 0.1 μF capacitor as close as possible to the supply pins.

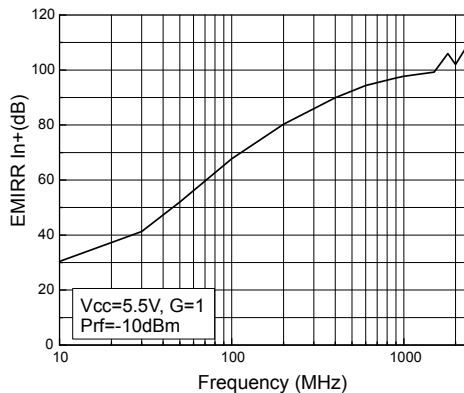
A good decoupling has several advantages for an application. First, it helps to reduce electromagnetic interference. Due to the modulation of the chopper, the decoupling capacitance also helps to reject the small ripple that may appear on the output.

TSZ121, TSZ122, and TSZ124 devices have been optimized for use with 10 $\text{k}\Omega$ in the feedback loop. With this, or a higher value of resistance, these devices offer the best performance.

5.10 EMI rejection ration (EMIRR)

The electromagnetic interference (EMI) rejection ratio, or EMIRR, describes the EMI immunity of operational amplifiers. An adverse effect that is common to many op amps is a change in the offset voltage as a result of RF signal rectification.

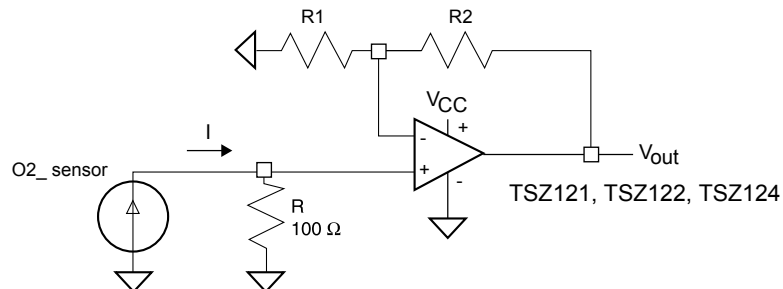
The TSZ121, TSZ122, and TSZ124 have been specially designed to minimize susceptibility to EMIRR and show an extremely good sensitivity. [Figure 46. EMIRR on IN+ pin](#) shows the EMIRR IN+ of the TSZ121, TSZ122, and TSZ124 measured from 10 MHz up to 2.4 GHz.

Figure 46. EMIRR on IN+ pin

5.11 Application examples

5.11.1 Oxygen sensor

The electrochemical sensor creates a current proportional to the concentration of the gas being measured. This current is converted into voltage thanks to R resistance. This voltage is then amplified by TSZ121, TSZ122, and TSZ124 devices (see [Figure 47. Oxygen sensor principle schematic](#)).

Figure 47. Oxygen sensor principle schematic

The output voltage is calculated using [Equation 2](#):

Equation 2

$$V_{\text{out}} = (I \times R - V_{\text{io}}) \times \left(\frac{R_2}{R_1} + 1 \right)$$

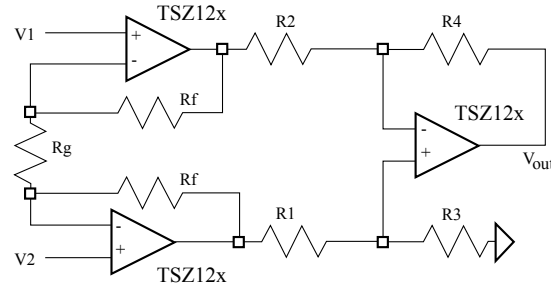
As the current delivered by the O₂ sensor is extremely low, the impact of the V_{io} can become significant with a traditional operational amplifier. The use of the chopper amplifier of the TSZ121, TSZ122, or TSZ124 is perfect for this application.

In addition, using TSZ121, TSZ122, or TSZ124 devices for the O₂ sensor application ensures that the measurement of O₂ concentration is stable even at different temperature thanks to a very good ΔV_{io}/ΔT.

5.11.2 Precision instrumentation amplifier

The instrumentation amplifier uses three op amps. The circuit, shown in [Figure 48. Precision instrumentation amplifier schematic](#), exhibits high input impedance, so that the source impedance of the connected sensor has no impact on the amplification.

Figure 48. Precision instrumentation amplifier schematic



The gain is set by tuning the R_g resistor. With $R_1 = R_2$ and $R_3 = R_4$, the output is given by [Section 5.11.2 Equation 3](#).

Equation 3

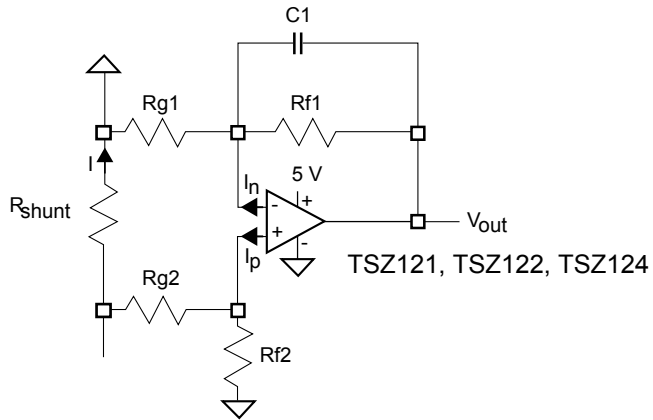
$$V_{out} = \left(V_2 - V_1 \right) \left[\frac{R_4}{R_2} \cdot \frac{2R_f}{R_g} + 1 \right]$$

The matching of R_1 , R_2 and R_3 , R_4 is important to ensure a good common mode rejection ratio (CMR).

5.11.3 Low-side current sensing

Power management mechanisms are found in most electronic systems. Current sensing is useful for protecting applications. The low-side current sensing method consists of placing a sense resistor between the load and the circuit ground. The resulting voltage drop is amplified using TSZ121, TSZ122, and TSZ124 devices (see [Figure 49. Low-side current sensing schematic](#)).

Figure 49. Low-side current sensing schematic



V_{out} can be expressed as follows:

Equation 4

$$V_{out} = R_{shunt} \times I \left(1 - \frac{R_{g2}}{R_{g2} + R_{f2}} \right) \left(1 + \frac{R_{f1}}{R_{g1}} \right) + I_p \left(\frac{R_{g2} \times R_{f2}}{R_{g2} + R_{f2}} \right) \times \left(1 + \frac{R_{f1}}{R_{g1}} \right) - I_n \times R_{f1} - V_{io} \left(1 + \frac{R_{f1}}{R_{g1}} \right)$$

Assuming that $R_{f2} = R_{f1} = R_f$ and $R_{g2} = R_{g1} = R_g$, [Equation 4](#) can be simplified as follows:

Equation 5

$$V_{out} = R_{shunt} \times I \left(\frac{R_f}{R_g} \right) - V_{io} \left(1 + \frac{R_f}{R_g} \right) + R_f \times I_{io}$$

The main advantage of using the chopper of the TSZ121, TSZ122, and TSZ124, for a low-side current sensing, is that the errors due to V_{io} and I_{io} are extremely low and may be neglected.

Therefore, for the same accuracy, the shunt resistor can be chosen with a lower value, resulting in lower power dissipation, lower drop in the ground path, and lower cost.

Particular attention must be paid on the matching and precision of R_{g1} , R_{g2} , R_{f1} , and R_{f2} , to maximize the accuracy of the measurement.

6

Package information

In order to meet environmental requirements, ST offers these devices in different grades of ECOPACK® packages, depending on their level of environmental compliance. ECOPACK® specifications, grade definitions and product status are available at: www.st.com. ECOPACK® is an ST trademark.

6.1 SC70-5 (or SOT323-5) package information

Figure 50. SC70-5 (or SOT323-5) package outline

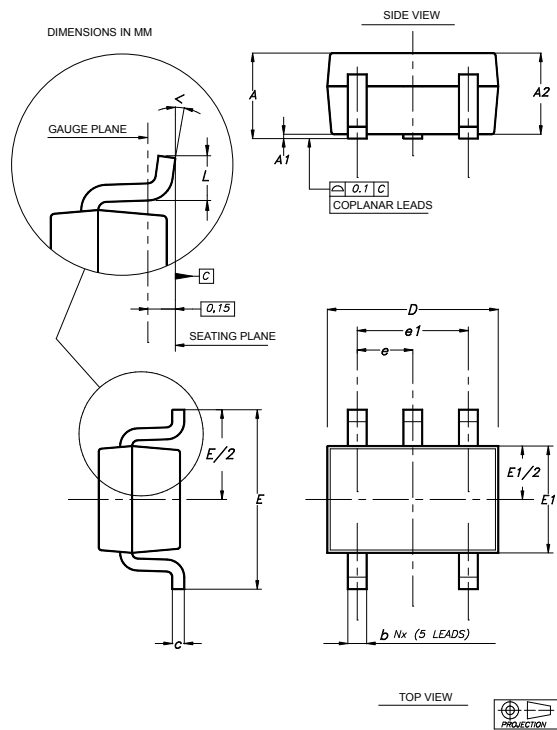


Table 6. SC70-5 (or SOT323-5) mechanical data

| Ref. | Dimensions | | | | | |
|------|-------------|------|------|--------|-------|-------|
| | Millimeters | | | Inches | | |
| | Min. | Typ. | Max. | Min. | Typ. | Max. |
| A | 0.80 | | 1.10 | 0.032 | | 0.043 |
| A1 | | | 0.10 | | | 0.004 |
| A2 | 0.80 | 0.90 | 1.00 | 0.032 | 0.035 | 0.039 |
| b | 0.15 | | 0.30 | 0.006 | | 0.012 |
| c | 0.10 | | 0.22 | 0.004 | | 0.009 |
| D | 1.80 | 2.00 | 2.20 | 0.071 | 0.079 | 0.087 |
| E | 1.80 | 2.10 | 2.40 | 0.071 | 0.083 | 0.094 |
| E1 | 1.15 | 1.25 | 1.35 | 0.045 | 0.049 | 0.053 |
| e | | 0.65 | | | 0.025 | |
| e1 | | 1.30 | | | 0.051 | |
| L | 0.26 | 0.36 | 0.46 | 0.010 | 0.014 | 0.018 |
| < | 0° | | 8° | 0° | | 8° |

6.2 SOT23-5 package information

Figure 51. SOT23-5 package outline

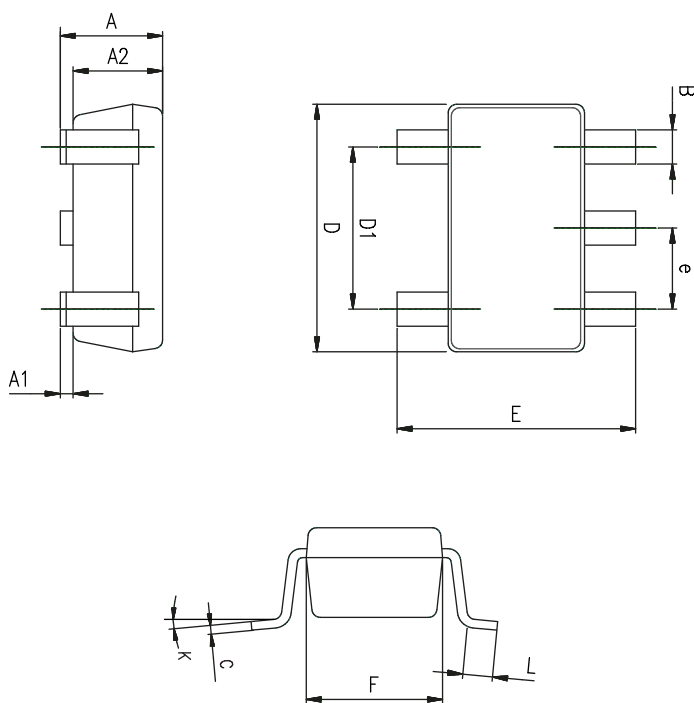


Table 7. SOT23-5 mechanical data

| Ref. | Dimensions | | | | | |
|------|-------------|------|------------|-----------|-------|------------|
| | Millimeters | | | Inches | | |
| | Min. | Typ. | Max. | Min. | Typ. | Max. |
| A | 0.90 | 1.20 | 1.45 | 0.035 | 0.047 | 0.057 |
| A1 | | | 0.15 | | | 0.006 |
| A2 | 0.90 | 1.05 | 1.30 | 0.035 | 0.041 | 0.051 |
| B | 0.35 | 0.40 | 0.50 | 0.014 | 0.016 | 0.020 |
| C | 0.09 | 0.15 | 0.20 | 0.004 | 0.006 | 0.008 |
| D | 2.80 | 2.90 | 3.00 | 0.110 | 0.114 | 0.118 |
| D1 | | 1.90 | | | 0.075 | |
| e | | 0.95 | | | 0.037 | |
| E | 2.60 | 2.80 | 3.00 | 0.102 | 0.110 | 0.118 |
| F | 1.50 | 1.60 | 1.75 | 0.059 | 0.063 | 0.069 |
| L | 0.10 | 0.35 | 0.60 | 0.004 | 0.014 | 0.024 |
| K | 0 degrees | | 10 degrees | 0 degrees | | 10 degrees |

6.3 DFN8 2 x 2 package information

Figure 52. DFN8 2 x 2 package outline

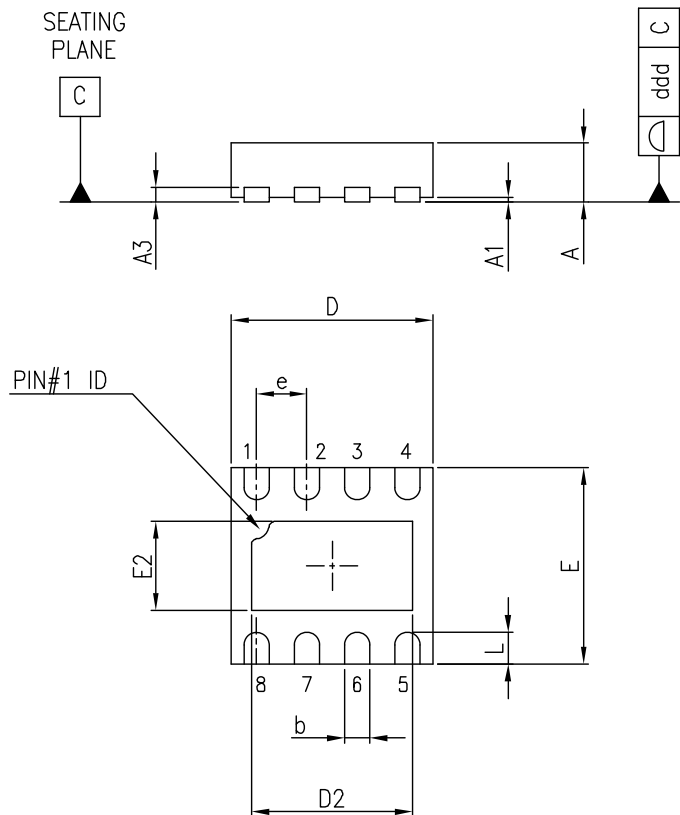
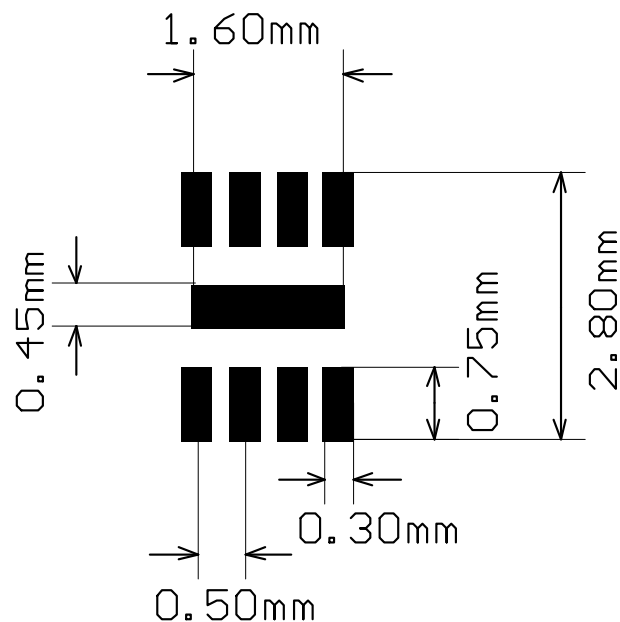


Table 8. DFN8 2 x 2 mechanical data

| Ref. | Dimensions | | | | | |
|------|-------------|-------|-------|--------|-------|-------|
| | Millimeters | | | Inches | | |
| | Min. | Typ. | Max. | Min. | Typ. | Max. |
| A | 0.51 | 0.55 | 0.60 | 0.020 | 0.022 | 0.024 |
| A1 | | | 0.05 | | | 0.002 |
| A3 | | 0.15 | | | 0.006 | |
| b | 0.18 | 0.25 | 0.30 | 0.007 | 0.010 | 0.012 |
| D | 1.85 | 2.00 | 2.15 | 0.073 | 0.079 | 0.085 |
| D2 | 1.45 | 1.60 | 1.70 | 0.057 | 0.063 | 0.067 |
| E | 1.85 | 2.00 | 2.15 | 0.073 | 0.079 | 0.085 |
| E2 | 0.75 | 0.90 | 1.00 | 0.030 | 0.035 | 0.039 |
| e | | 0.50 | | | 0.020 | |
| L | 0.225 | 0.325 | 0.425 | 0.009 | 0.013 | 0.017 |
| ddd | | | 0.08 | | | 0.003 |

Figure 53. DFN8 2 x 2 recommended footprint



6.4 MiniSO8 package information

Figure 54. MiniSO8 package outline

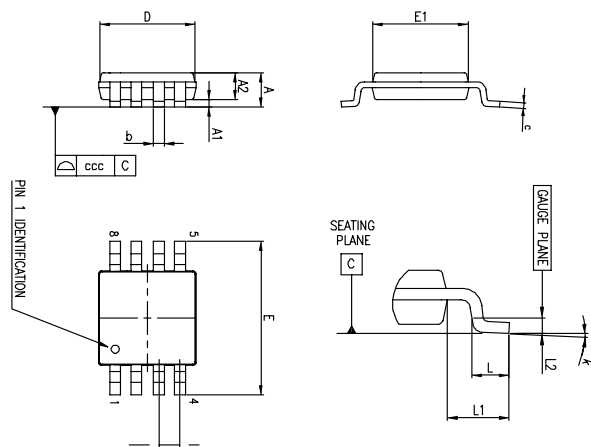


Table 9. MiniSO8 package mechanical data

| Ref. | Dimensions | | | | | |
|------|-------------|------|------|--------|-------|--------|
| | Millimeters | | | Inches | | |
| | Min. | Typ. | Max. | Min. | Typ. | Max. |
| A | | | 1.1 | | | 0.043 |
| A1 | 0 | | 0.15 | 0 | | 0.0006 |
| A2 | 0.75 | 0.85 | 0.95 | 0.030 | 0.033 | 0.037 |
| b | 0.22 | | 0.40 | 0.009 | | 0.016 |
| c | 0.08 | | 0.23 | 0.003 | | 0.009 |
| D | 2.80 | 3.00 | 3.20 | 0.11 | 0.118 | 0.126 |
| E | 4.65 | 4.90 | 5.15 | 0.183 | 0.193 | 0.203 |
| E1 | 2.80 | 3.00 | 3.10 | 0.11 | 0.118 | 0.122 |
| e | | 0.65 | | | 0.026 | |
| L | 0.40 | 0.60 | 0.80 | 0.016 | 0.024 | 0.031 |
| L1 | | 0.95 | | | 0.037 | |
| L2 | | 0.25 | | | 0.010 | |
| k | 0° | | 8° | 0° | | 8° |
| ccc | | | 0.10 | | | 0.004 |

6.5 SO8 package information

Figure 55. SO8 package outline

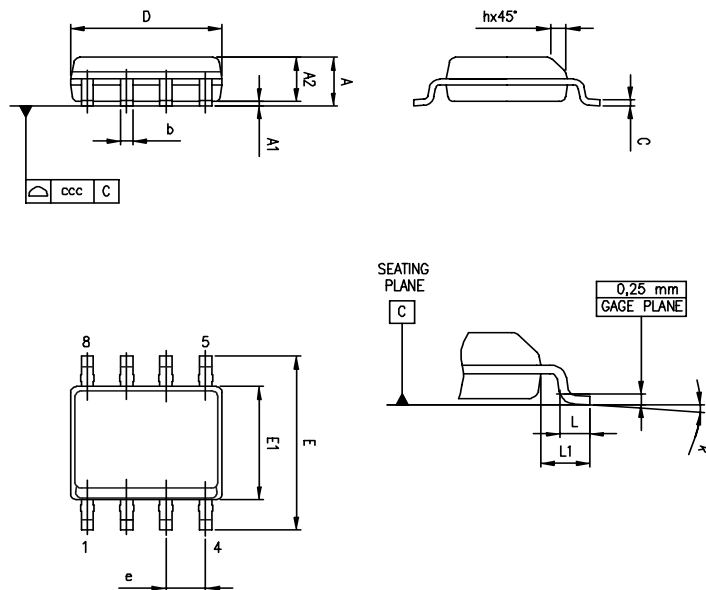


Table 10. SO8 package mechanical data

| Ref. | Dimensions | | | | | |
|------|-------------|------|------|--------|-------|-------|
| | Millimeters | | | Inches | | |
| | Min. | Typ. | Max. | Min. | Typ. | Max. |
| A | | | 1.75 | | | 0.069 |
| A1 | 0.10 | | 0.25 | 0.004 | | 0.010 |
| A2 | 1.25 | | | 0.049 | | |
| b | 0.28 | | 0.48 | 0.011 | | 0.019 |
| c | 0.17 | | 0.23 | 0.007 | | 0.010 |
| D | 4.80 | 4.90 | 5.00 | 0.189 | 0.193 | 0.197 |
| E | 5.80 | 6.00 | 6.20 | 0.228 | 0.236 | 0.244 |
| E1 | 3.80 | 3.90 | 4.00 | 0.150 | 0.154 | 0.157 |
| e | | 1.27 | | | 0.050 | |
| h | 0.25 | | 0.50 | 0.010 | | 0.020 |
| L | 0.40 | | 1.27 | 0.016 | | 0.050 |
| L1 | | 1.04 | | | 0.040 | |
| k | 0° | | 8° | 0° | | 8° |
| ccc | | | 0.10 | | | 0.004 |

6.6 QFN16 3x3 package information

Figure 56. QFN16 3x3 package outline

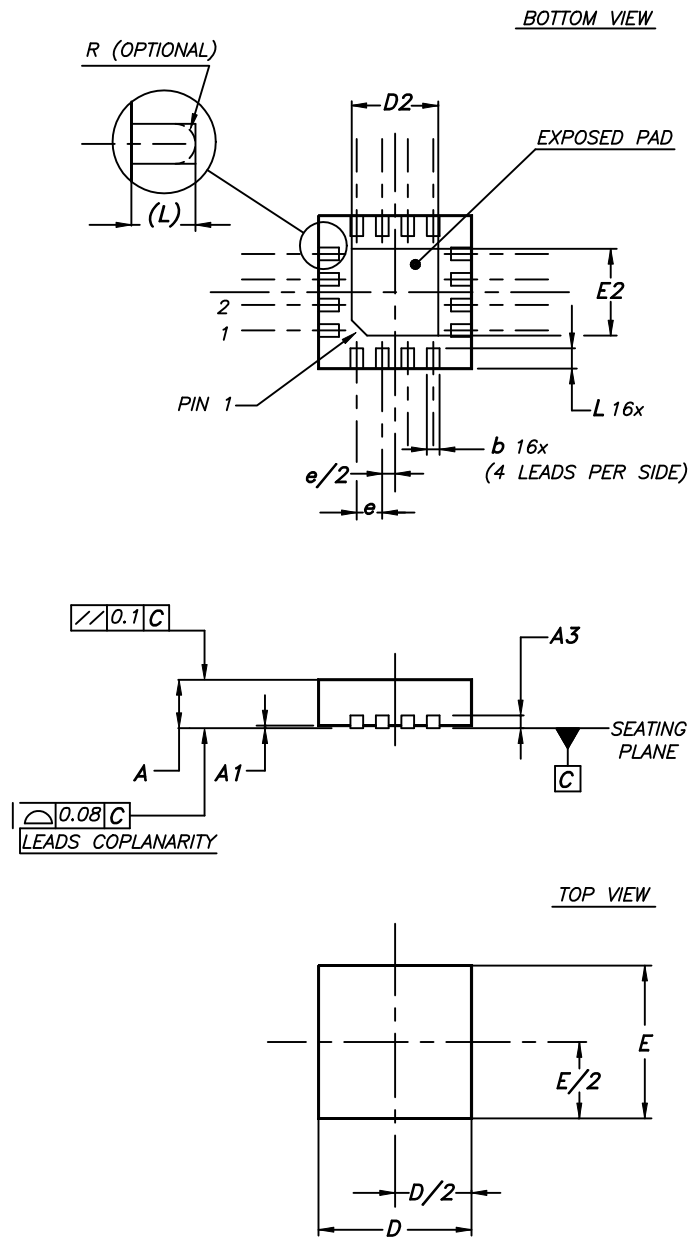
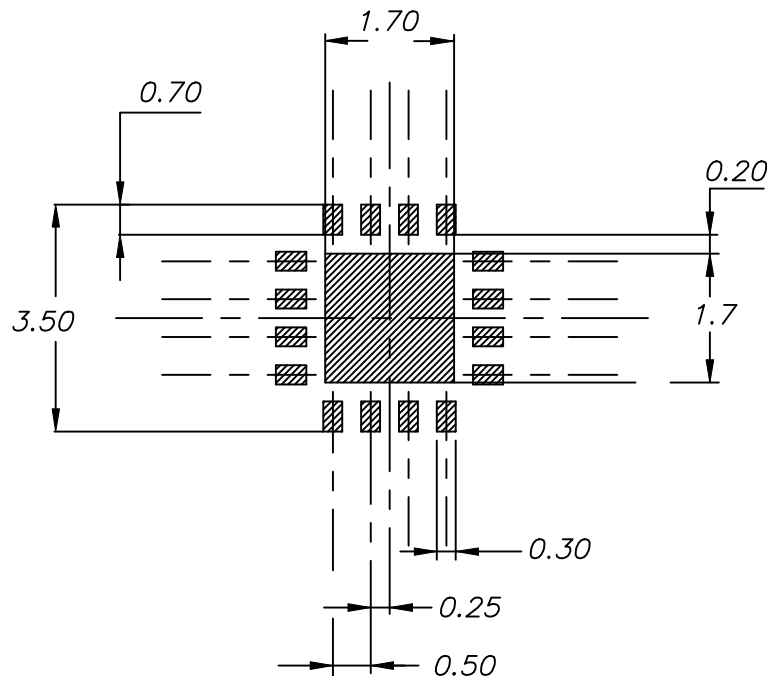


Table 11. QFN16 3x3 mechanical data

| Ref. | Dimensions | | | | | |
|------|-------------|------|------|--------|-------|-------|
| | Millimeters | | | Inches | | |
| | Min. | Typ. | Max. | Min. | Typ. | Max. |
| A | 0.80 | 0.90 | 1.00 | 0.031 | 0.035 | 0.039 |
| A1 | 0 | | 0.05 | 0 | | 0.002 |
| A3 | | 0.20 | | | 0.008 | |
| b | 0.18 | | 0.30 | 0.007 | | 0.012 |
| D | 2.90 | 3.00 | 3.10 | 0.114 | 0.118 | 0.122 |
| D2 | 1.50 | | 1.80 | 0.059 | | 0.071 |
| E | 2.90 | 3.00 | 3.10 | 0.114 | 0.118 | 0.122 |
| E2 | 1.50 | | 1.80 | 0.059 | | 0.071 |
| e | | 0.50 | | | 0.020 | |
| L | 0.30 | | 0.50 | 0.012 | | 0.020 |

Figure 57. QFN16 3x3 recommended footprint

6.7 TSSOP14 package information

Figure 58. TSSOP14 package outline

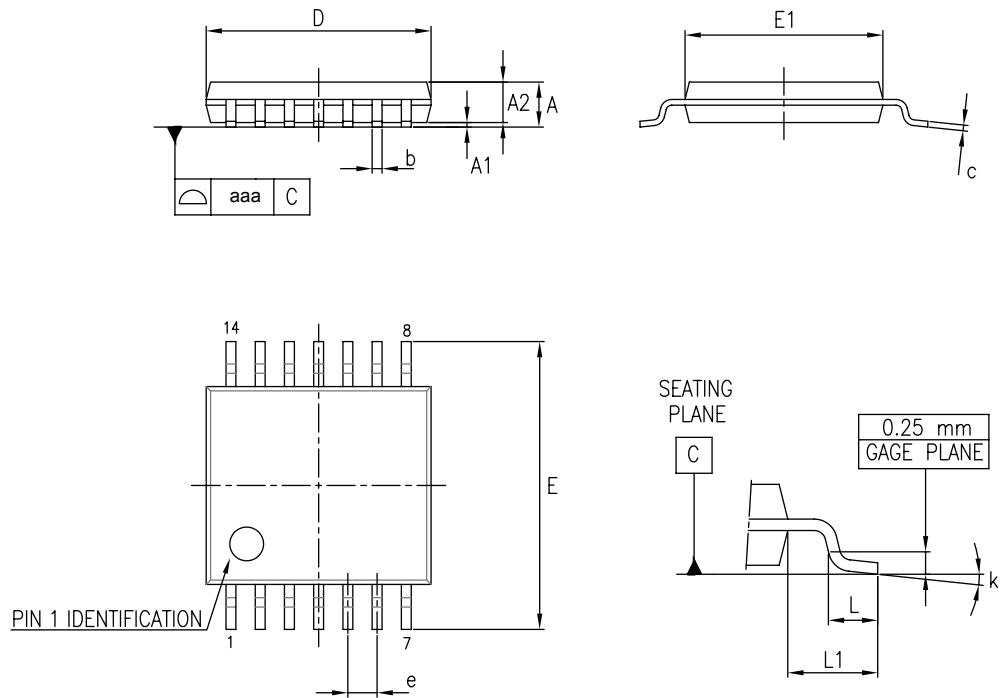


Table 12. TSSOP14 package mechanical data

| Ref. | Dimensions | | | | | |
|------|-------------|------|------|--------|--------|--------|
| | Millimeters | | | Inches | | |
| | Min. | Typ. | Max. | Min. | Typ. | Max. |
| A | | | 1.20 | | | 0.047 |
| A1 | 0.05 | | 0.15 | 0.002 | 0.004 | 0.006 |
| A2 | 0.80 | 1.00 | 1.05 | 0.031 | 0.039 | 0.041 |
| b | 0.19 | | 0.30 | 0.007 | | 0.012 |
| c | 0.09 | | 0.20 | 0.004 | | 0.0089 |
| D | 4.90 | 5.00 | 5.10 | 0.193 | 0.197 | 0.201 |
| E | 6.20 | 6.40 | 6.60 | 0.244 | 0.252 | 0.260 |
| E1 | 4.30 | 4.40 | 4.50 | 0.169 | 0.173 | 0.176 |
| e | | 0.65 | | | 0.0256 | |
| L | 0.45 | 0.60 | 0.75 | 0.018 | 0.024 | 0.030 |
| L1 | | 1.00 | | | 0.039 | |
| k | 0° | | 8° | 0° | | 8° |
| aaa | | | 0.10 | | | 0.004 |

7

Ordering information

Table 13. Order codes

| Order code | Temperature range | Package | Packaging | Marking |
|---------------------------|-------------------|-----------|---------------|----------|
| TSZ121ICT | -40 to 125 °C | SC70-5 | Tape and reel | K44 |
| TSZ121ILT | | SOT23-5 | | K143 |
| TSZ122IQ2T | | DFN8 2x2 | | K33 |
| TSZ122IST | | MiniSO8 | | K208 |
| TSZ122IDT | | SO8 | | TSZ122I |
| TSZ124IQ4T | | QFN16 3x3 | | K193 |
| TSZ124IPT | | TSSOP14 | | TSZ124I |
| TSZ121IYLT ⁽¹⁾ | | SOT23-5 | | K192 |
| TSZ122IYDT ⁽¹⁾ | | SO8 | | K192D |
| TSZ122IYST ⁽¹⁾ | | MiniSO8 | | K192 |
| TSZ124IYPT ⁽¹⁾ | | TSSOP14 | | TSZ124IY |

1. Qualified and characterized according to AEC Q100 and Q003 or equivalent, advanced screening according to AEC Q001 & Q002 or equivalent.

Revision history

Table 14. Document revision history

| Date | Revision | Changes |
|-------------|----------|-----------------------------------------------------------------------------------------------------------------------------------------------------------------------------------------------------------------------------------------------------------------------------------------------------------------------------------------------------------------------------------------------------------------------------------------------------------------------------------------------------------------------------------------------------------------------------------------------------------------------------------------------------------------------------------------------------------------------------------------------------------------------------------------------------------------------------------------------------------------------------------------------------------------------------------------------------------------------------------------------------------------------------------------------------------------------------------------------------------|
| 16-Aug-2012 | 1 | Initial release. |
| 25-Apr-2013 | 2 | <p>Added dual and quad products (TSZ122 and TSZ124 respectively)</p> <p>Updated title</p> <p>Added following packages: DFN8 2x2, MiniSO8, QFN16 3x3, TSSOP14</p> <p>Updated Features</p> <p>Added Benefits and Related products</p> <p>Updated Description</p> <p>Updated Table 1 (R_{thja}, ESD)</p> <p>Updated Table 3 (V_{io}, $\Delta V_{io}/\Delta T$, CMR, A_{vd}, ICC, e_n, and C_s)</p> <p>Updated Table 4 (V_{io}, $\Delta V_{io}/\Delta T$, CMR, I_{CC}, e_n, and C_s)</p> <p>Updated Table 5 (V_{io}, $\Delta V_{io}/\Delta T$, CMR, SVR, EMIRR, I_{CC}, t_s, e_n, and C_s)</p> <p>Updated curves of Section 3: Electrical characteristics</p> <p>Added Section 4.7: Capacitive load</p> <p>Small update Section 4.9: Optimized application recommendation (capacitor)</p> <p>Added Section 4.10: EMI rejection ration (EMIRR)</p> <p>Updated Table 10: Order codes</p> |
| 11-Sep-2013 | 3 | <p>Added SO8 package for commercial part number TSZ122IDT</p> <p>Related products: added hyperlinks for TSV71x and TSV73x products</p> <p>Table 1: updated CDM information</p> <p>Figure 6, Figure 7: updated X-axes titles</p> <p>Figure 12: updated X-axis and Y-axis titles</p> <p>Figure 19: updated title</p> <p>Figure 26: updated X-axis (logarithmic scale)</p> <p>Figure 27 and Figure 28: updated Y-axis titles</p> |
| 23-May-2014 | 4 | <p>Table 1: updated ESD information</p> <p>Table 5: added footnote 3</p> <p>Table 10: Order codes: added automotive qualification footnotes 1 and 2; updated marking of TSZ122IST.</p> <p>Updated disclaimer</p> |
| 09-May-2016 | 5 | <p>Updated document layout</p> <p>Table 13: "Order codes": added new automotive grade order code TSZ122IYD, updated footnotes of other automotive grade order codes.</p> |
| 07-Feb-2017 | 6 | Table 3, Table 4, and Table 5: added parameter "Low-frequency peak-to-peak input noise" (e_n). Figure 26: "0.1 Hz to 10 Hz noise": updated legend (0.75 μ Vpp instead of 0.2 μ Vpp) |
| 12-Apr-2017 | 7 | Updated footnote related to TSZ122IYDT in Table 13: "Order codes". Minor changes throughout the document. |
| 18-May-2017 | 8 | Updated package outline drawing and mechanical data in Section 6.2: SOT23-5 package information. |
| 12-Nov-2018 | 9 | Updated Figure 43. Stability criteria with a serial resistor at $V_{DD} = 5$ V and Figure 44. Stability criteria with a serial resistor at $V_{DD} = 1.8$ V |
| 26-Feb-2019 | 10 | Updated Figure 43. Stability criteria with a serial resistor at $V_{DD} = 5$ V and Figure 44. Stability criteria with a serial resistor at $V_{DD} = 1.8$ V |

Contents

| | | |
|-------------------|----------------------------------------------------------------|-----------|
| 1 | Package pin connections | 2 |
| 2 | Absolute maximum ratings and operating conditions | 3 |
| 3 | Electrical characteristics..... | 4 |
| 4 | Electrical characteristic curves | 8 |
| 5 | Application information..... | 14 |
| 5.1 | Operation theory | 14 |
| 5.1.1 | Time domain | 14 |
| 5.1.2 | Frequency domain | 15 |
| 5.2 | Operating voltages | 15 |
| 5.3 | Input pin voltage ranges..... | 15 |
| 5.4 | Rail-to-rail input..... | 16 |
| 5.5 | Input offset voltage drift over temperature | 16 |
| 5.6 | Rail-to-rail output..... | 16 |
| 5.7 | Capacitive load | 16 |
| 5.8 | PCB layout recommendations..... | 17 |
| 5.9 | Optimized application recommendation | 17 |
| 5.10 | EMI rejection ration (EMIRR)..... | 17 |
| 5.11 | Application examples | 18 |
| 5.11.1 | Oxygen sensor | 18 |
| 5.11.2 | Precision instrumentation amplifier | 18 |
| 5.11.3 | Low-side current sensing | 19 |
| 6 | Package information..... | 21 |
| 6.1 | SC70-5 (or SOT323-5) package information | 22 |
| 6.2 | SOT23-5 package information..... | 22 |
| 6.3 | DFN8 2 x 2 package information..... | 23 |
| 6.4 | MiniSO8 package information | 26 |
| 6.5 | SO8 package information..... | 26 |
| 6.6 | QFN16 3x3 package information..... | 27 |
| 6.7 | TSSOP14 package information..... | 29 |

| | |
|-------------------------------------|-----------|
| 7 Ordering information | 31 |
| Revision history | 32 |
| Contents | 33 |
| List of tables | 35 |
| List of figures..... | 36 |

List of tables

| | | |
|------------------|--------------------------------------------------------------------------------------------------------------------------------------------------------------------------------------------------------------|----|
| Table 1. | Absolute maximum ratings (AMR) | 3 |
| Table 2. | Operating conditions | 3 |
| Table 3. | Electrical characteristics at $V_{CC+} = 1.8$ V with $V_{CC-} = 0$ V, $V_{icm} = V_{CC}/2$, $T = 25^\circ C$, and $R_L = 10\text{ k}\Omega$ connected to $V_{CC}/2$ (unless otherwise specified) | 4 |
| Table 4. | Electrical characteristics at $V_{CC+} = 3.3$ V with $V_{CC-} = 0$ V, $V_{icm} = V_{CC}/2$, $T = 25^\circ C$, and $R_L = 10\text{ k}\Omega$ connected to $V_{CC}/2$ (unless otherwise specified) | 5 |
| Table 5. | Electrical characteristics at $V_{CC+} = 5$ V with $V_{CC-} = 0$ V, $V_{icm} = V_{CC}/2$, $T = 25^\circ C$, and $R_L = 10\text{ k}\Omega$ connected to $V_{CC}/2$ (unless otherwise specified) | 6 |
| Table 6. | SC70-5 (or SOT323-5) mechanical data | 22 |
| Table 7. | SOT23-5 mechanical data | 23 |
| Table 8. | DFN8 2 x 2 mechanical data | 24 |
| Table 9. | MiniSO8 package mechanical data | 26 |
| Table 10. | SO8 package mechanical data | 27 |
| Table 11. | QFN16 3x3 mechanical data | 29 |
| Table 12. | TSSOP14 package mechanical data | 30 |
| Table 13. | Order codes | 31 |
| Table 14. | Document revision history | 32 |

List of figures

| | | |
|-------------------|---------------------------------------------------------------------------------|----|
| Figure 1. | Pin connections for each package (top view) | 2 |
| Figure 2. | Supply current vs. supply voltage | 8 |
| Figure 3. | Input offset voltage distribution at $V_{CC} = 5\text{ V}$ | 8 |
| Figure 4. | Input offset voltage distribution at $V_{CC} = 3.3\text{ V}$ | 8 |
| Figure 5. | Input offset voltage distribution at $V_{CC} = 1.8\text{ V}$ | 8 |
| Figure 6. | V_{IO} temperature co-efficient distribution (-40 °C to 25 °C) | 8 |
| Figure 7. | V_{IO} temperature co-efficient distribution (25 °C to 125 °C) | 8 |
| Figure 8. | Input offset voltage vs. supply voltage | 9 |
| Figure 9. | Input offset voltage vs. input common-mode at $V_{CC} = 1.8\text{ V}$ | 9 |
| Figure 10. | Input offset voltage vs. input common-mode at $V_{CC} = 2.7\text{ V}$ | 9 |
| Figure 11. | Input offset voltage vs. input common-mode at $V_{CC} = 5.5\text{ V}$ | 9 |
| Figure 12. | Input offset voltage vs. temperature | 9 |
| Figure 13. | V_{OH} vs. supply voltage | 9 |
| Figure 14. | V_{OL} vs. supply voltage | 10 |
| Figure 15. | Output current vs. output voltage at $V_{CC} = 1.8\text{ V}$ | 10 |
| Figure 16. | Output current vs. output voltage at $V_{CC} = 5.5\text{ V}$ | 10 |
| Figure 17. | Input bias current vs. common mode at $V_{CC} = 5\text{ V}$ | 10 |
| Figure 18. | Input bias current vs. common mode at $V_{CC} = 1.8\text{ V}$ | 10 |
| Figure 19. | Input bias current vs. temperature at $V_{CC} = 5\text{ V}$ | 10 |
| Figure 20. | Bode diagram at $V_{CC} = 1.8\text{ V}$ | 11 |
| Figure 21. | Bode diagram at $V_{CC} = 2.7\text{ V}$ | 11 |
| Figure 22. | Bode diagram at $V_{CC} = 5.5\text{ V}$ | 11 |
| Figure 23. | Open loop gain vs. frequency | 11 |
| Figure 24. | Positive slew rate vs. supply voltage | 11 |
| Figure 25. | Negative slew rate vs. supply voltage | 11 |
| Figure 26. | 0.1 Hz to 10 Hz noise | 12 |
| Figure 27. | Noise vs. frequency | 12 |
| Figure 28. | Noise vs. frequency and temperature | 12 |
| Figure 29. | Output overshoot vs. load capacitance | 12 |
| Figure 30. | Small signal | 12 |
| Figure 31. | Large signal | 12 |
| Figure 32. | Positive overvoltage recovery at $V_{CC} = 1.8\text{ V}$ | 13 |
| Figure 33. | Positive overvoltage recovery at $V_{CC} = 5\text{ V}$ | 13 |
| Figure 34. | Negative overvoltage recovery at $V_{CC} = 1.8\text{ V}$ | 13 |
| Figure 35. | Negative overvoltage recovery at $V_{CC} = 5\text{ V}$ | 13 |
| Figure 36. | PSRR vs. frequency | 13 |
| Figure 37. | Output impedance vs. frequency | 13 |
| Figure 38. | Block diagram in the time domain (step 1) | 14 |
| Figure 39. | Block diagram in the time domain (step 2) | 14 |
| Figure 40. | V_{IO} cancellation principle | 15 |
| Figure 41. | Block diagram in the frequency domain | 15 |
| Figure 42. | Input current limitation | 16 |
| Figure 43. | Stability criteria with a serial resistor at $V_{DD} = 5\text{ V}$ | 17 |
| Figure 44. | Stability criteria with a serial resistor at $V_{DD} = 1.8\text{ V}$ | 17 |
| Figure 45. | Test configuration for Riso | 17 |
| Figure 46. | EMIRR on IN+ pin | 18 |
| Figure 47. | Oxygen sensor principle schematic | 18 |
| Figure 48. | Precision instrumentation amplifier schematic | 19 |
| Figure 49. | Low-side current sensing schematic | 19 |

| | | |
|-------------------|------------------------------------------------|----|
| Figure 50. | SC70-5 (or SOT323-5) package outline | 22 |
| Figure 51. | SOT23-5 package outline | 23 |
| Figure 52. | DFN8 2 x 2 package outline | 24 |
| Figure 53. | DFN8 2 x 2 recommended footprint | 25 |
| Figure 54. | MiniSO8 package outline | 26 |
| Figure 55. | SO8 package outline | 27 |
| Figure 56. | QFN16 3x3 package outline | 28 |
| Figure 57. | QFN16 3x3 recommended footprint | 29 |
| Figure 58. | TSSOP14 package outline | 30 |

IMPORTANT NOTICE – PLEASE READ CAREFULLY

STMicroelectronics NV and its subsidiaries ("ST") reserve the right to make changes, corrections, enhancements, modifications, and improvements to ST products and/or to this document at any time without notice. Purchasers should obtain the latest relevant information on ST products before placing orders. ST products are sold pursuant to ST's terms and conditions of sale in place at the time of order acknowledgement.

Purchasers are solely responsible for the choice, selection, and use of ST products and ST assumes no liability for application assistance or the design of Purchasers' products.

No license, express or implied, to any intellectual property right is granted by ST herein.

Resale of ST products with provisions different from the information set forth herein shall void any warranty granted by ST for such product.

ST and the ST logo are trademarks of ST. All other product or service names are the property of their respective owners.

Information in this document supersedes and replaces information previously supplied in any prior versions of this document.

© 2019 STMicroelectronics – All rights reserved